RSC Advances

COMMUNICATION

Cite this: *RSC Adv.*, 2014, **4**, 2648

Received 9th August 2013
Accepted 7th November 2013

DOI: 10.1039/c3ra46233a

www.rsc.org/advances

Experimental assessment of physical upper limit for hydrogen storage capacity at 20 K in densified MIL-101 monoliths†

Hyunchul Oh,[a] Dan Lupu,[b] Gabriela Blanita[b] and Michael Hirscher*[a]

The physical upper limit of hydrogen uptake for powder and compressed pellet MIL-101 has been experimentally investigated. Maximum uptake in pellets at 20 K achieves 9.6 wt% and 42 g L^{-1}. Moreover, cryo-adsorption of hydrogen on pellets compared to liquid H_2 possesses a larger temperature window for operation without boil-off loss, which will be beneficial for industrial applications.

The development of hydrogen storage technologies for mobile applications still requires overcoming some technical barriers to meet the DoE revised targets for 2017. An efficient on-board hydrogen storage system requires 0.055 kg H_2 per kg system and 0.040 kg H_2 per L system, gravimetric and volumetric capacity, respectively. The analysis of hydrogen storage options for light-duty vehicles concluded that some options can meet several of the intermediate targets but not all the targets simultaneously.[1]

A recent analysis demonstrated[2] that, even though liquid hydrogen is frequently considered too energetically intensive for large scale transportation, the high cost of delivering, compression and compressed storage compensates for the high cost of liquefaction. Furthermore, dispensing liquid H_2 at the station is faster, and a compact high-pressure cryogenic system possesses an enhanced storage capacity.[3]

An alternative to cryo-compression is the physisorption in porous materials at more moderate temperatures and pressures.[4] The high gravimetric storage capacity and low heat evolution during loading of porous metal-organic frameworks represents a huge step forward to materials for hydrogen-storage systems based on cryo-adsorption.[5] Two of the most promising porous material classes for a hydrogen cryo-adsorption tank, activated carbon (AX-21_33) and metal-organic framework (MOF-5, MOF-177), have been investigated in the pressure range up to 2 MPa and at temperatures from 77 K to 125 K and at room temperature.[1,3,6]

Taking into account the reported advantages of refuelling cryogenic pressure vessels operating down to 20 K,[2,3] H_2 adsorption data at this temperature for high capacity sorbents are also needed to assess the potential of meeting the gravimetric and volumetric capacity targets for on-board H_2 storage systems based on cryo-adsorption. In particular, compressed pellets of high capacity sorbents which can be compacted without significant loss of hydrogen storage capacity have attracted much attention due to a huge enhancement of the volumetric hydrogen capacity. Recently, several densified monoliths of MOFs (*e.g.* MOF-5, MOF-177 and MIL-101) have been reported.[7,8,9] Among those, MIL-101-Cr can be considered as a promising adsorbent due to the high stability toward moisture (H_2O)[10] compared to Zn-based MOFs.[11]

In this study, the cryo-adsorption (20 K) of H_2 in the compressed pellets and powder of MIL-101 is explored by high-resolution low-pressure isotherms, and the physical upper limit of hydrogen storage capacity is determined experimentally. Furthermore, the 20 K cryo-adsorption storage system is compared with low pressure liquid hydrogen (LH_2) system in terms of operating temperature.

The textural properties of the MIL-101 compressed pellet and powder samples were analyzed by nitrogen and hydrogen adsorption at 77 K and 19.5 K, respectively (see Fig. 1, Table 1 and ESI†). The fully reversible hydrogen isotherms for pellets and powders at 19.5 K exhibit the characteristic IUPAC type-I adsorption isotherm, which is typical for microporous materials. In order to determine the appropriate BET pressure range for microporous materials, two consistency criteria should be followed;[12] (1) the straight line fitted to the BET plot must have a positive intercept, and (2) the pressure range should be chosen so that $\nu_{ads}(1 - P/P_0)$ is always increasing with P/P_0 as shown in Fig. S2–5, ESI.† Additionally, the most important parameter for BET calculations from H_2 adsorption isotherms at near boiling point is the cross-sectional area of the probe molecule (H_2), which is a function of the density of the adsorbed phase.

[a]*Max Planck Institute for Intelligent Systems, Heisenbergstrasse 3, D-70569 Stuttgart, Germany. E-mail: hirscher@is.mpg.de*

[b]*National Institute for Research and Development of Isotopic and Molecular Technologies, 65-103 Donath Str., 400293 Cluj-Napoca, Romania*

† Electronic supplementary information (ESI) available: Experimental details, PXRD, N_2 BET, volumetric H_2 uptake calculation. See DOI: 10.1039/c3ra46233a

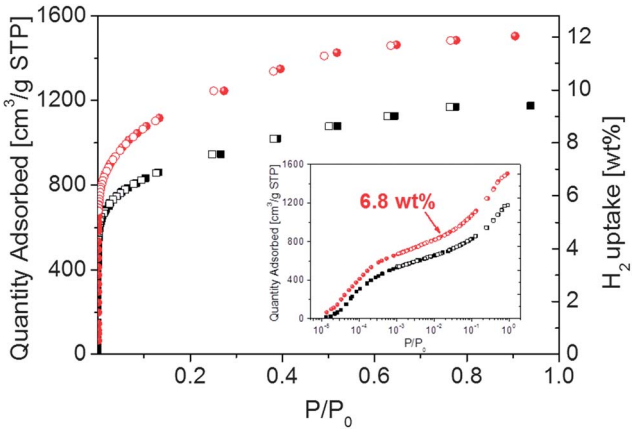

Fig. 1 Low-pressure high-resolution hydrogen adsorption (closed symbol)/desorption (open symbol) isotherms at 19.5 K for powder (circle red) and compressed pellet (square black) of MIL-101. (inset) Semi-logarithmic isotherm plot of H_2 at 19.5 K on MIL-101 which resolve the pore filling steps.

Therefore, the cross-sectional area of hydrogen (A_{H_2}) is calculated for hexagonal closest packing of the bulk liquid with a molecular volume of 28.4 $cm^3\ mol^{-1}$ (20 K) which yields A_{H_2} = 14.2 $Å^2$. The device set-up and calculation details are well presented in detail elsewhere.[13] According to this approach, the calculated hydrogen BET specific surface area (SSA) for pellets and powders have been determined to 2919 $m^2\ g^{-1}$ and 3780 $m^2\ g^{-1}$, respectively. The nitrogen BET (pellets: 2745 $m^2\ g^{-1}$ and powders: 3414 $m^2\ g^{-1}$) exhibits slightly smaller SSAs than hydrogen BET due to the different size of the probe molecules.[12]

For hydrogen storage purposes in porous MOF sorbents system, it is important to evaluate the physical upper limit of storage capacity at high filling of hydrogen in order to fully assess the potential of its specific application. Typically in literature, the experimental hydrogen capacity is reported either as excess or absolute capacity. Here, we use the "excess uptake" for hydrogen storage capacity, which is also considered as a theoretical upper limit for storage capacity at 20 K, 1 bar. In this regards, the hydrogen capacity can be defined as adsorbed hydrogen mass per unit weight (gravimetric) or volume (volumetric).[7]

From adsorption isotherms at 19.5 K shown in Fig. 1, the textural characteristics of adsorbent (MIL-101) for powder and pellet are reported in Table 1, and analysed as follows:

(1) For the degassed pellet with envelope density of 0.4 g cm^{-3}, 1 L contains 400 g MIL-101. With the excess uptake from Table 1, this corresponds to 42.3 g L^{-1} volumetric capacity. The total volumetric storage capacity may be even higher because within the pellet there are still 0.5 $cm^3\ g^{-1}$ available for gas, as shown in ESI.

(2) The case of hypothetical 'single crystal' MIL-101 (degassed crystal density 0.43 g cm^{-3}, or 430 g L^{-1} as evaluated in ESI), the measured value for powder leads to 58.1 g L^{-1} volumetric capacity at saturation.

It is also worth to be noted that the obtained gravimetric hydrogen uptake at 19.5 K (11.9 wt% for powder MIL-101) in this work is almost twice higher than the excess uptake of powder MIL-101 at 77 K reported in literature (mostly below 6 wt%[9,14,15]). Since the linear relationship exists between excess hydrogen uptake and SSA (also known as Chahine's rule: 1 wt% per 500$m^2\ g^{-1}$), the hydrogen storage capacity of 6.8 wt % can be expected based on N_2 BET (3414 $m^2\ g^{-1}$). Thus, the rest of hydrogen storage capacity (5.1 wt%) among maximum uptake (11.9 wt%) can be ascribed to the hydrogen pore filling by condensation in large cavities (largest pore size: 34 Å) of MIL-101. This is in line with adsorption isotherm in a logarithmic representation of pressure (inset of Fig. 1) showing two steps with the hydrogen adsorption increasing exponentially above 6.8 wt% (red arrow), indicating pore filling of cavities. It is of importance to note that the significant difference in storage capacity between 20 K and 77 K is a clear evidence for a correlation between hydrogen uptake at high loading and pore volume.[16] In addition, this cryogenic low-pressure isotherm near its boiling point allows us to predict the theoretical maximum (or physical limit) of hydrogen storage capacity (which is in good agreement with simulation results reported in ref. 15), and thus also shows that the gravimetric storage capacity of powder MIL-101 at 77 K can be enhanced up to 100% by pore condensation at 20 K compared to 77 K.

Hydrogen sorption isobar measurement; Temperature dependent pressure change

Hydrogen storage method for today's fuel cell vehicles is mostly based on the compressed of gases at typically 35 or 70 MPa. However, even at these high pressures the energy density of hydrogen still falls far short of the DOE 2017 targets. As an alternative to compression, hence, the density of hydrogen can

Table 1 Textural characteristics of the MIL-101 compressed pellet and powder samples determined from nitrogen and hydrogen adsorption/desorption isotherms[a]

Type	N_2 SSA ($m^2\ g^{-1}$)	H_2 SSA ($m^2\ g^{-1}$)	Total SPV_{H_2} (P/P_0 = 0.9) ($cm^3\ g^{-1}$)	Envelope density (g cm^{-3})	Excess H_2 uptake: 77 K, 58 bar[9] wt%	19.5 K, P/P_0 = 0.9: $cm^3\ g^{-1}$	mg g^{-1}	wt%	g L^{-1}
Powder	3414	3780	1.9	—	5.82	1503	135.2	11.9	—
Pellet	2745	2919	1.5	0.4	4.75	1176	105.7	9.6	42.3

[a] N_2 SSA: nitrogen BET specific surface area at 77 K (P/P_0 = 0.02–0.1), H_2 SSA: hydrogen BET specific surface area at 19.5 K (P/P_0 = 0.02-0.1), total SPV_{H_2}: total pore volume from hydrogen BET at 0.9 P/P_0, envelope density: degassed sample mass per pellet volume.

be also increased by liquefaction at 20 K. These low pressure liquid hydrogen storage systems have high density and reasonably low cost,[17] but this method also face a technical difficulty (*i.e.* evaporative losses after a short dormancy; boil-off). In order to overcome boil-off effects, therefore, new approach that combines two storage technologies (hybrid system; liquefaction at 20 K with cryo-adsorption) might be beneficial for capturing the advantage of both systems.

Fig. 2 shows the influence of temperature change in the hydrogen storage system. In this investigation, the activated material in the sample holder is loaded with 1069 mbar hydrogen at room temperature and the connection valve is closed so that the volume available for the gas remains constant. Then, the sample holder is cooled to approximately 14 K where hydrogen is liquid. The pressure is monitored while the sample is heated to different intermediate temperatures; each temperature is kept constant for approximately 2 min at which point the pressure is recorded. For the empty sample holder, the pressure is almost 0 mbar at around 15 K as the hydrogen in the sample holder is liquefied. Slightly above 16 K the phase transition from liquid to gaseous is observed by a sudden increase of the pressure in the sample holder. Then, the slope becomes smaller with increasing temperature (above 20 K) as the hydrogen remains in the gaseous phase and the pressure increases only due to thermal expansion. With MIL101 compressed pellet in the sample holder, the pressure develops differently. The pressure remains constant (~0 mbar) up to approximately 37 K. Afterwards, the pressure increase smoothly as a sigmoidal shape until approximately 160 K. Thereafter the pressure matches nearly that of the empty sample holder.

The steep increase of pressure in empty holder at slightly over 20 K represents the boil-off effect. Hence, any vessel system that store liquid hydrogen will inevitably have some heat leaks that cause vaporization of the LH_2, leading to pressurization of the tank if liquid hydrogen is stored in a closed vessel. This is a very critical issue for mobile applications, therefore, the LH_2 storage system is currently limited to space applications (where the hydrogen is consumed in a rather short time). However, this sudden hydrogen expansion can be prevented by adding an adsorbent. Owing to the van der Waals force between guest molecule and surface, hydrogen gas remains in adsorbed phase up to 37 K, and pressure develop gradually as a sigmoidal shape even at higher T. This is very important point to be noted while designing a storage system because the operating temperature range can be significantly enhanced from 20 K up to 37 K (which is above the critical point of H_2, $T_c = 32.98$ K) by simply adding sorbents (MIL-101). Furthermore, the temperature tolerance of phase transition (from fully adsorbed phase at 37 K to fully gas at 160 K) is also very high (*ca.* ~120 K) while the empty vessel possesses only a temperature tolerance of 4 K (from fully liquid at 16 K to fully gas at 20 K).

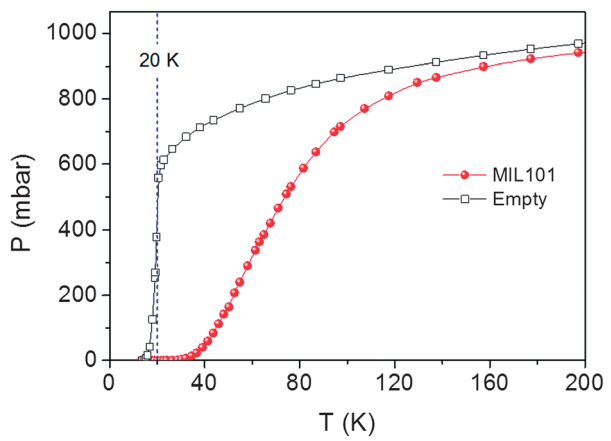

Fig. 2 Pressure change in the sample holder with temperature variation (black square: the empty sample holder, red circle: sample holder containing compressed pellet of MIL-101.

Conclusions

The present study provides experimental evidence that saturation uptake for microporous materials possessing large cavities at high loading is strongly related to the pore filling of large cavities. By using cryogenic low-pressure isotherms near its boiling point, the physical upper limit of hydrogen uptake for powder and compressed pellet MIL101 samples have been experimentally investigated. This maximum hydrogen excess adsorption of pelletized MIL-101 has been determined to 9.6 wt % and 42.3 g L^{-1} (19.5 K, $P/P_0 = 0.9$), suggesting a promising adsorbent candidate for achieving the volumetric and gravimetric storage system target established by the U.S. Department of Energy for 2017 (5.5 wt% and 40 g L^{-1}). Moreover, cryo-adsorption on MIL-101 pellets at 20 K could be beneficial for industrial applications compared to liquid H_2 due to the larger temperature window for operation without boil-off loss (up to 37 K: above the critical point of H_2, Tc = 32.98 K).The conclusions section should come at the end of the article.

Acknowledgements

H. Oh is grateful for the scholarship from the International Max Planck Research School for Advanced Materials (IMPRS-AM). Partial funding by the German Research Foundation DFG within the priority program SSP 1362 and by a grant of the Romanian National Authority for Scientific Research, CNCS-UEFISCDI with project number PN-II-ID-PCE-2011-3-0350 is gratefully acknowledged. Part of this work was supported by COST Action on "Nanostructured materials for solid-state hydrogen storage".

Notes and references

1 R. K. Ahluwalia, T. Q. Hua and J. K. Peng, *Int. J. Hydrogen Energy*, 2012, **37**, 2891–2910.
2 M. D. Paster, R. K. Ahluwalia, G. Berry, A. Elgowainy, S. Lasher, K. McKenney and M. Gardiner, *Int. J. Hydrogen Energy*, 2011, **36**, 14534–14551.
3 S. M. Aceves, G. Petitpas, F. Espinosa-Loza, M. J. Matthews and E. Ledesma-Orozco, *Int. J. Hydrogen Energy*, 2013, **38**, 2480–2489.
4 B. Hardy, C. Corgnale, R. Chahine, M.-A. Richard, S. Garrison, D. Tamburello, D. Cossement and D. Anton, *Int. J. Hydrogen Energy*, 2012, **37**, 5691–5705.

5 M. Hirscher, *Angew. Chem. Int. Ed.*, 2011, **50**, 581–582.
6 M. Schlichtenmayer, B. Streppel and M. Hirscher, *Int. J. Hydrogen Energy*, 2011, **36**, 586–591.
7 R. Zacharia, D. Cossement, L. Lafi and R. Chahine, *J. Mater. Chem.*, 2010, **20**, 2145–2151.
8 J. J. Purewal, D. Liu, J. Yang, A. Sudik, D. J. Siegel, S. Maurer and U. Müller, *Int. J. Hydrogen Energy*, 2012, **37**, 2723–2727.
9 O. Ardelean, G. Blanita, G. Borodi, M. D. Lazar, I. Misan, I. Coldea and D. Lupu, *Int. J. Hydrogen Energy*, 2013, **38**, 7046–7055.
10 G. Férey, C. Mellot-Draznieks, C. Serre, F. Millange, J. Dutour, S. Surblé and I. Margiolaki, *Science*, 2005, **309**, 2040–2042.
11 J. J. Low, A. I. Benin, P. Jakubczak, J. F. Abrahamian, S. A. Faheem and R. R. Willis, *J. Am. Chem. Soc.*, 2009, **131**, 15834–15842.
12 T. Düren, F. Millange, G. Férey, K. S. Walton and R. Q. Snurr, *J. Phys. Chem. C*, 2007, **111**, 15350–15356.
13 B. Streppel and M. Hirscher, *Phys. Chem. Chem. Phys.*, 2011, **13**, 3220–3222.
14 M. Latroche, S. Surble, C. Serre, C. Mellot-Draznieks, P. L. Llewellyn, J. H. Lee, J. S. Chang, S. H. Jhung and G. Ferey, *Angew. Chem. Int. Ed.*, 2006, **45**, 8227–8231.
15 A. Ghoufi, J. Deschamps and G. Maurin, *J. Phys. Chem. C*, 2012, **116**, 10504–10509.
16 K. S. Walton and R. Q. Snurr, *J. Am. Chem. Soc.*, 2007, **129**, 8552–8556.
17 F. A. G. Krainz, *SAE Technical Paper 2006-01-0432*, 2006, DOI: 10.4271/2006-01-0432.